

UCLA

UCLA Previously Published Works

Title

Four-dimensional Multiphase Steady-State MRI with Ferumoxytol Enhancement: Early Multicenter Feasibility in Pediatric Congenital Heart Disease.

Permalink

<https://escholarship.org/uc/item/53q4v6g3>

Journal

Radiology, 300(1)

ISSN

0033-8419

Authors

Nguyen, Kim-Lien
Ghosh, Reena M
Griffin, Lindsay M
et al.

Publication Date

2021-07-01

DOI

10.1148/radiol.2021203696

Peer reviewed

Four-dimensional Multiphase Steady-State MRI with Ferumoxytol Enhancement: Early Multicenter Feasibility in Pediatric Congenital Heart Disease




Kim-Lien Nguyen, MD • Reena M. Ghosh, MD • Lindsay M. Griffin, MD • Takegawa Yoshida, MD • Arash Bedayat, MD • Cynthia K. Rigsby, MD • Mark A. Fogel, MD • Kevin K. Whitehead, MD • Peng Hu, MD • J. Paul Finn, MD

From the Diagnostic Cardiovascular Imaging Laboratory, Department of Radiological Sciences (K.L.N., T.Y., A.B., P.H., J.P.F.), and Division of Cardiology (K.L.N.), David Geffen School of Medicine at UCLA, 300 Medical Plaza, B119, Los Angeles, CA 90095; VA Greater Los Angeles Healthcare System, Los Angeles, Calif (K.L.N.); Division of Cardiology, Children's Hospital of Philadelphia, Philadelphia, Pa (R.M.G., M.A.F., K.K.W.); Department of Medical Imaging, Ann & Robert H. Lurie Children's Hospital, Chicago, Ill (L.M.G., C.K.R.); and Department of Radiology, Northwestern University Feinberg School of Medicine, Chicago, Ill (L.M.G., C.K.R.). Received September 12, 2020; revision requested October 28; revision received February 3, 2021; accepted February 8. Address correspondence to J.P.F. (e-mail: jpfinn@mednet.ucla.edu).

Supported by the National Heart, Lung, and Blood Institute (grant R01HL127153). K.L.N. supported by American Heart Association grant 18TPA34170049, VA-MERIT grant 101-CX001901, and National Institutes of Health grant R01HL148182. R.M.G. supported by National Institutes of Health grant T32GM008562. L.M.G. supported by American Heart Association grant 19TPA34850066. C.K.R. supported by National Institutes of Health grant R01HL115828 and American Heart Association grant 19TPA34850066. M.A.F. supported by National Institutes of Health grants R01HL149139 and R01HL142142. P.H. supported by National Institutes of Health grants R01HL127153 and R01HL148182, VA-MERIT grant 101-CX001901, and American Heart Association grant 18TPA34170049. J.P.F. supported by National Institutes of Health grants R01HL127153 and R01HL148182 and American Heart Association grant 18TPA34170049.

Conflicts of interest are listed at the end of this article.

See also the editorial by Roest and Lamb in this issue.

Radiology 2021; 300:162–173 • <https://doi.org/10.1148/radiol.2021203696> • Content codes:   

Background: The value of MRI in pediatric congenital heart disease (CHD) is well recognized; however, the requirement for expert oversight impedes its widespread use. Four-dimensional (4D) multiphase steady-state imaging with contrast enhancement (MUSIC) is a cardiovascular MRI technique that uses ferumoxytol and captures all anatomic features dynamically.

Purpose: To evaluate multicenter feasibility of 4D MUSIC MRI in pediatric CHD.

Materials and Methods: In this prospective study, participants with CHD underwent 4D MUSIC MRI at 3.0 T or 1.5 T between 2014 and 2020. From a pool of 460 total studies, an equal number of MRI studies from three sites ($n = 60$) was chosen for detailed analysis. With use of a five-point scale, the feasibility of 4D MUSIC was scored on the basis of artifacts, image quality, and diagnostic confidence for intracardiac and vascular connections ($n = 780$). Respiratory motion suppression was assessed by using the signal intensity profile. Bias between 4D MUSIC and two-dimensional (2D) cine imaging was evaluated by using Bland-Altman analysis; 4D MUSIC examination duration was compared with that of the local standard for CHD.

Results: A total of 206 participants with CHD underwent MRI at 3.0 T, and 254 participants underwent MRI at 1.5 T. Of the 60 MRI examinations chosen for analysis (20 per site; median participant age, 14.4 months [interquartile range, 2.3–49 months]; 33 female participants), 56 (93%) had good or excellent image quality scores across a spectrum of disease complexity (mean score \pm standard deviation: 4.3 ± 0.6 for site 1, 4.9 ± 0.3 for site 2, and 4.6 ± 0.7 for site 3; $P < .001$). Artifact scores were inversely related to image quality ($r = -0.88$, $P < .001$) and respiratory motion suppression ($P < .001$, $r = -0.45$). Diagnostic confidence was high or definite in 730 of 780 (94%) intracardiac and vascular connections. The correlation between 4D MUSIC and 2D cine ventricular volumes and ejection fraction was high (range of $r = 0.72$ – 0.85 ; $P < .001$ for all). Compared with local standard MRI, 4D MUSIC reduced the image acquisition time (44 minutes \pm 20 vs 12 minutes \pm 3, respectively; $P < .001$).

Conclusion: Four-dimensional multiphase steady-state imaging with contrast enhancement MRI in pediatric congenital heart disease was feasible in a multicenter setting, shortened the examination time, and simplified the acquisition protocol, independently of disease complexity.

Clinical trial registration no. NCT02752191

©RSNA, 2021

Online supplemental material is available for this article.

Although the benefits of MRI in pediatric congenital heart disease (CHD) are well established, unpredictable examination times and the need for expert interactive supervision limit its widespread use. Researchers have proposed several technically sophisticated MRI strategies to accelerate volumetric acquisition (1–3) and shorten examination times (4,5). However, implementation of new techniques often faces bottlenecks due to the requirement for specialized in-house reconstruction, postprocessing, and,

ultimately, whether a research agreement exists between the MRI vendor and the local institution. As controversies surrounding gadolinium retention in brain and bone diminish enthusiasm for gadolinium-enhanced MRI, alternative approaches for contrast-enhanced or noncontrast imaging have become more attractive, particularly in small children who will undergo repeated imaging over their lifetime. Ferumoxytol MRI using the four-dimensional (4D) multiphase steady-state imaging with contrast enhancement

Abbreviations

bSSFP = balanced steady-state fast precession, CHD = congenital heart disease, 4D = four-dimensional, MUSIC = multiphase steady-state imaging with contrast enhancement, 3D = three-dimensional, 2D = two-dimensional

Summary

Ferumoxylol-enhanced MRI using the pulse sequence four-dimensional multiphase steady-state imaging with contrast enhancement was feasible in a multicenter setting, shortened the examination time, and simplified imaging in pediatric congenital heart disease.

Key Results

- In an evaluation of 60 study participants at three centers using ferumoxylol-enhanced MRI and the four-dimensional multiphase steady-state imaging with contrast enhancement (MUSIC) pulse sequence in pediatric congenital heart disease (CHD), 93% of examinations (56 of 60) had image quality scores of good or excellent.
- Of intracardiac and vascular connections, 730 of 780 (94%) had diagnostic confidence scores of high or definite across a spectrum of CHD complexity.
- MUSIC reduced the image acquisition time for evaluation of cardiac function and vascular connections compared to that with conventional MRI (mean, 12 minutes \pm 3 vs 44 minutes \pm 20, respectively; $P < .001$).

(MUSIC) pulse sequence produces isotropic, high-spatial-resolution, cardiac phase-resolved three-dimensional (3D) images independent of disease complexity (6,7). Cardiac and respiratory-gated MRI data are acquired during uninterrupted positive pressure ventilation, and image reconstruction is completed in-line within seconds. Reconstructed images become immediately available for two-dimensional (2D) cine interrogation in arbitrary planes with use of any commercial software with Digital Imaging and Communications in Medicine viewing capability.

Four-dimensional MUSIC MRI relies on the steady-state distribution properties of ferumoxylol for enhanced intravascular signal intensity. Ferumoxylol is an ultrasmall superparamagnetic iron oxide nanoparticle that has been approved by the U.S. Food and Drug Administration for clinical treatment of iron deficiency anemia. Because of its long intravascular half-life and high relaxivity (8,9), ferumoxylol is uniquely effective. The use of ferumoxylol is not without hypersensitivity risks; however, to date, the safety profile for diagnostic use of ferumoxylol has been favorable (8,9). In a single-center study, 4D MUSIC MRI provided highly diagnostic images (6,10,11) and added value in the care of patients with CHD (10,12). In this study, we aimed to assess the feasibility of use of 4D MUSIC in pediatric CHD when distributed geographically across multiple academic medical centers and operating at different magnetic field strengths.

Materials and Methods

The local institutional review board approved this Health Insurance Portability and Accountability Act-compliant, prospective, multicenter observational study (ClinicalTrials.gov identifier: NCT02752191). All participants or their guardians gave informed consent. Detailed methodology is provided in Appendix E1 (online).

Study Sites and Participants

Study sites were quaternary CHD referral centers ($n = 3$) in the United States. Each site prospectively enrolled consecutive pediatric patients with CHD who underwent 4D MUSIC MRI between 2014 and 2020 for clinically indicated reasons. Inclusion criteria were pediatric patients with CHD referred for ferumoxylol-enhanced 4D MUSIC MRI under general anesthesia and assent for participation in research. Exclusion criteria included known sensitivity to intravenous iron products, multiple drug allergies, history of iron overload or conditions that may be associated with iron overload, and dysrhythmias. Enrollment of the final participant cohort is detailed in Figure E1 (online). Briefly, between January 2014 and July 2020, a total of 460 participants with CHD (age range, 1 day to 19 years) underwent 4D MUSIC MRI at 3.0 T ($n = 206$) or 1.5 T ($n = 254$). Twenty participants from each site ($n = 60$) were selected for detailed image analysis. Because of the heterogeneity of CHD, we defined three categories, as follows: group 1, simple CHD (native and/or repaired, with patient cared for by the general medical community); group 2, CHD of moderate severity (with patients seen periodically at regional CHD centers); and group 3, CHD of great complexity (with patients seen regularly at CHD centers of excellence) (13).

Previously published work on multicenter safety of ferumoxylol in MRI (14) included the 60 participants evaluated in this current study. That report focused on the safety of off-label diagnostic use of ferumoxylol in MRI, whereas the current study evaluated the implementation of 4D MUSIC in pediatric CHD at three medical centers.

Four-dimensional MUSIC MRI Implementation and Image Acquisition

Site 3 implemented 4D MUSIC at 3.0 T (in 2014; Siemens) and distributed the pulse sequence to sites 1 and 2 (1.5 T, in 2017; Siemens). Key technical details for the 4D MUSIC pulse sequence have been previously described (6), and additional details are provided in Appendix E1 (online). Briefly, 4D MUSIC is a 3D, cardiac phase-resolved, electrocardiographically triggered, spoiled gradient-echo sequence performed during uninterrupted positive pressure ventilation and uses the continuously monitored airway pressure signal for respiratory gating (Fig 1). Typical pulse sequence parameters, magnet strength, and coils used at each site are summarized in Table 1. The ferumoxylol dose (Feraheme, AMAG Pharmaceuticals) ranged between 3 and 4 mg iron per kilogram. The minimum repetition time for each line of k-space was 3 msec or less and the echo time was 1 msec or less, with a receiver bandwidth of 800–870 Hz per pixel. Cartesian k-space sampling was used, and acceleration was limited to parallel acquisition with generalized autocalibrating partial parallel acquisition (maximum acceleration factor of 3). Before image acquisition, we diluted ferumoxylol by a factor of 10 in normal saline and infused the solution during approximately 10–12 minutes. Participants were intubated and sedated with general anesthesia throughout the MRI examination. Individual sites also performed 2D balanced steady-state fast precession (bSSFP) cine for validation purposes.

Technologists and nursing staff continuously monitored the participant's vital signs throughout the examination. We used predefined definitions (10) for adverse reactions.

Framework for Evaluation

Technical implementation and workflow.—We collected information regarding hardware, software, scanning parameters, use of anesthesia, technologist level of expertise, onboarding time, local MRI protocol for participants with CHD, and image acquisition time before and after implementation of 4D MUSIC MRI. The duration of 4D MUSIC MRI examinations was calculated as the time from the start to the end of the 4D MUSIC image acquisition. Because 4D MUSIC examinations provide cine and angiographic images, we calculated the duration of local conventional CHD MRI examinations by computing the total time needed to acquire cine and MR angiographic images. We did not include the time required for acquisition of localizer images for both 4D MUSIC and local conventional CHD MRI.

Image analysis: image quality and artifacts.—To minimize selection bias, each site randomly chose 20 4D MUSIC MRI examinations from a list of participants enrolled in the study, anonymized the examinations, and submitted them to the core laboratory for detailed image analysis. One core laboratory investigator (T.Y., with 5 years of research experience) who was not involved in grading the images deidentified the originating site of the submitted examinations. Three investigators (A.B., K.L.N., J.P.F., with 5, 7, and more than 20 years of cardiovascular MRI experience, respectively) were blinded to the study site. In two successive sessions that were 2–3 weeks apart, the investigators graded the examinations ($n = 60$) for overall image quality; artifacts; and visualization of the valves, hepatic veins, pulmonary vessels, and coronary vessels by using a five-point Likert scale (Table 2). Disagreements were resolved by consensus (K.L.N., J.P.F.). The signal intensity profile at the lung-diaphragm-liver interface was plotted (ImageJ 1.52n, National Institutes of Health), and the signal intensity slope was used as a proxy for respiratory motion control.

Image analysis: diagnostic confidence.—Local investigators (R.M.G., L.M.G., and A.B., each with more than 5

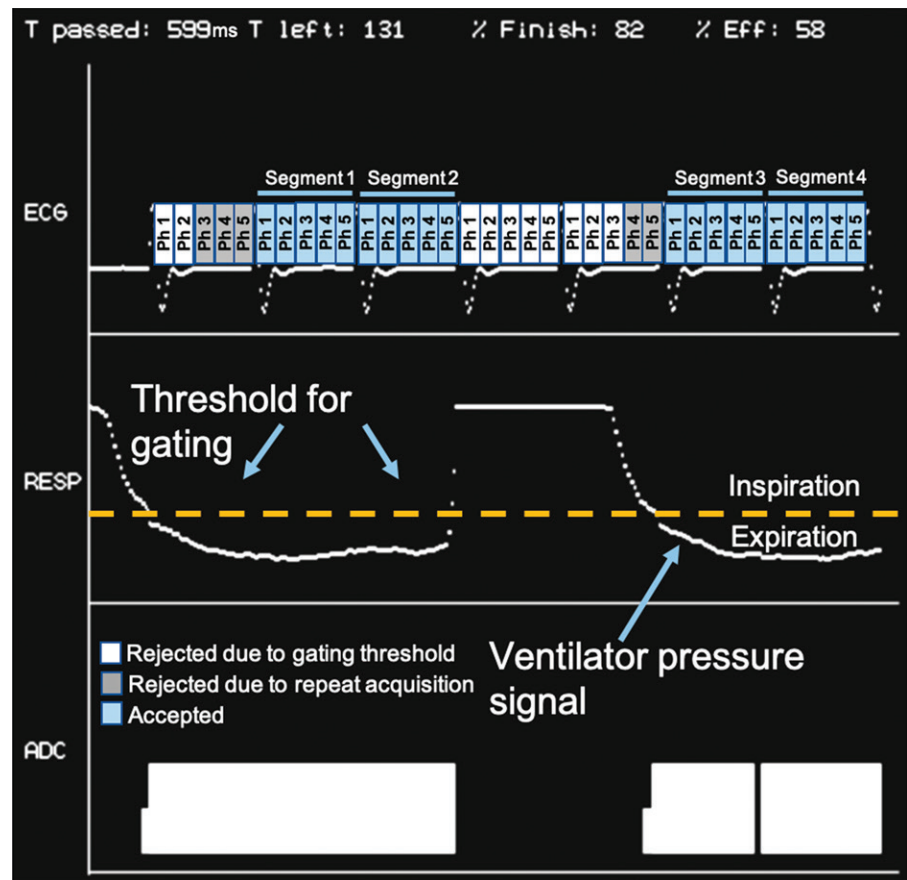


Figure 1: Illustration shows electrocardiographically triggered (ECG) and respiratory-gated (RESP) four-dimensional (4D) multiphase steady-state imaging with contrast enhancement (MUSIC) pulse sequence. Three-dimensional data acquisition for 4D MUSIC employs Cartesian k-space readout with k-space segmentation (analogous to two-dimensional cine MRI) in phase-encoding directions. The number of k-space lines in each segment of k-space is user-definable and determines duration of cardiac phase (and therefore temporal resolution). To optimize efficiency of respiratory gating, the decision to accept or reject k-space data was made at the level of each cardiac phase (k-space segment) rather than each R-R interval and was based on ventilator pressure signal corresponding to that k-space segment. Electrocardiographic signal and tracing of ventilator pressure signal are shown to demonstrate segmented, respiratory-gated 4D MUSIC image acquisition. In this example, gating efficiency (Eff) is approximately 57% (four of seven heartbeats) at 82% completion. ADC = analog digital conversion, Ph = phase, T = time.

years of cardiovascular MRI experience) were blinded to all clinical information including correlative imaging data; they scored the examinations (20 per site) for diagnostic confidence across 13 anatomic categories (normal vs abnormal) of intracardiac and vascular connections. Each local investigator used a scale of 1–5 (1 = no confidence, 2 = guessing, 3 = moderate, 4 = high, 5 = definite) to indicate the level of confidence. After grading the diagnostic confidence, local readers adjudicated the MRI findings with locally available echocardiographic, catheterization, and operative data. Each site provided quantitative ventricular volumes and ejection fractions from multi-section 2D bSSFP cine. The core laboratory reformatted the corresponding 4D MUSIC MRI findings from all sites into multi-section 2D cine images (3–4 mm section thickness, zero intersection gap) and quantified the 4D MUSIC–derived ventricular volumes and ejection fractions (Medis Suite MR, Medis Medical Imaging Systems).

Table 1: Comparison of Technical Implementation and Examination Duration across All Sites

Parameter	Site 1	Site 2	Site 3
4D MUSIC MRI			
Magnet field strength	1.5 T	1.5 T	3.0 T
Coil type	Body, flex, clamshell	Body, flex, head/neck	Body, flex, head/neck
MRI software platform	VD13	VD13, VE11C	VD13, VE11C
Image analysis	Vitrea (Vital Images), Medis Suite	Circle CVI42	Osirix, Medis, Circle CVI42, Mimics (Materialise), Vitrea
Pulse sequence version	MUSIC v11c (Siemens)	MUSIC v11c (Siemens)	MUSIC v11c (Siemens)
Scanning parameters			
TR/TE (msec)	2.96/1.04	2.25/1.12	3.3/1.09
Flip angle (degrees)	30	25	25
Spatial resolution (mm)	1.5	0.9–1.1	0.6–0.9
Temporal resolution (msec)	38	20–45	43
Cardiac phases	9	12–20	9–12
Anesthesia			
Neuromuscular relaxant	Yes	Yes	Yes
General anesthesia	Yes	Yes	Yes
Sedation only	No	Yes	No
Technologist experience	Cardiovascular MRI	Cardiovascular MRI	Cardiovascular MRI
Local physicist support	Yes	No	Yes
Start-up time	1–2 sessions	30 min × 5 examinations	Parent site
Local standard MRI			
Function and morphologic characteristics	2D cine bSSFP	2D cine bSSFP	2D cine bSSFP
Flow	2D PC, 4D PC	2D PC	2D PC
MRA	TWIST, IR FLASH	TWIST, IR FLASH	TWIST, 3D T1-weighted SGRE
Imaging time (min)			
Image acquisition time for local standard (2D cine, MRA)*†	52 ± 20 (23–112)	34 ± 8 (16–52)	51 ± 20 (24–109)
Image acquisition time for 4D MUSIC MRI*†	13 ± 3 (7–21)	12 ± 2 (9–20)	11 ± 4 (7–21)
Image postprocessing time (cardiac function)	Unchanged	Unchanged	Unchanged
Physician supervision time			
With 4D MUSIC MRI	None	None	None
Without 4D MUSIC MRI†	52 ± 20	34 ± 8	51 ± 20

Note.—bSSFP = balanced steady-state free precession, FLASH = fast low-angle single-shot, 4D = four-dimensional, IR = inversion recovery, MRA = MR angiography, MUSIC = multiphase steady-state imaging with contrast enhancement, PC = phase contrast, SGRE = spoiled gradient echo, TE = echo time, TR = repetition time, TWIST = time-resolved angiography with interleaved stochastic trajectories, 2D = two-dimensional.

* Image acquisition time for local MRI standard accounts only for 2D cine and MRA acquisition because 4D MUSIC MRI acquires cine images for function, morphologic characteristics, and angiography. Image acquisition times do not include localizer images. Numbers in parentheses are the range.

† Data are means ± standard deviations.

Statistical Analysis

We used MedCalc software (version 18, MedCalc Software) for statistical analyses. We tested the data for normality by using the D’Agostino test. Data are summarized as frequencies and percentages. Descriptive statistics are reported as range, means ± standard deviations, or medians and interquartile range. We used two-factor analysis of variance with repeated measures to compare the overall image quality and artifacts across the three centers. Spearman rank correlations and multiple regression models were used to evaluate relationships among magnet field strength, overall image quality, image artifacts, and signal intensity slope at the lung-diaphragm-liver interface. The paired Student *t* test was used to compare image acquisition time for the local

standard MRI and 4D MUSIC MRI. By using Spearman rank correlation and Bland-Altman analyses, we evaluated the correlation and bias between 2D bSSFP cine- and 4D MUSIC-derived ventricular volumetry and ejection fraction. Bonferroni correction was used to account for multiple comparisons. *P* < .05 was considered to indicate a statistically significant difference.

Results

Participant and Site Characteristics

Figure E1 (online) is a flow diagram for selection of study participants. Of the 460 participants who underwent 4D MUSIC MRI, 60 (13%; 20 per site; median age, 14.4 months [inter-

Table 2: Core Laboratory Image Quality Grading Scheme

Overall Image Quality Score	Artifacts	Valves	Hepatic Veins	Pulmonary Vessels	Coronary Arteries
5 = Excellent; sharp delineation of all relevant anatomic structures, excellent contrast, no artifacts	1 = No ghosting or cardiac motion blurring	Valve apparatus visualized in all phases. Valvular stenosis, leaflet thickening and motility evaluable	Third-order tributaries clearly visualized	Arteries and veins clearly visualized to third-order branches and tributaries	Origins and course clearly visualized
4 = Good; delineation of all intracardiac structures, minimal artifacts	2 = Mild ghosting or cardiac motion blurring on at least one phase	Valve apparatus visualized on most phases. Valvular stenosis and leaflet thickening evaluable	Second-order tributaries clearly visualized	Arteries and veins clearly visualized to second-order branches and tributaries	Origins and proximal course clearly visualized
3 = Diagnostic; good delineation of all intracardiac structures, mild artifacts	3 = Mild ghosting and cardiac motion blurring limiting fine detail in some phases	Valve apparatus visualized in some phases. Valvular stenosis and leaflet thickening evaluable	Main hepatic veins clearly visualized	First-order branches and tributaries clearly visualized	Origins visualized with confidence
2 = Limited; limited delineation of several intracardiac structures, moderate artifacts	4 = Moderate ghosting and/or cardiac motion blurring limiting the assessment of several structures	Valve apparatus visualized in at least one phase	Main hepatic veins visualized but poorly defined	Main, right, and left artery and vein clearly visualized	One origin visualized
1 = Nondiagnostic; poor delineation of relevant anatomic structures, severe artifacts	5 = Severe ghosting and/or cardiac motion limiting the assessment of major intracardiac structures	Valve apparatus not visualized	Main hepatic veins not confidently evaluable	Main, right, and left and vein poorly visualized	Not seen

Note.—Artifacts include ghosting and cardiac motion. Valves include the aortic valve, mitral valve, pulmonic valve, and tricuspid valve.

quartile range, 2.3–49 months]; 33 female participants) were included in the current study and are summarized in Table 3. In general, participants at site 1 were older and larger, whereas participants at site 2 and site 3 were younger and smaller. Differences in age and body size among the sites reflect local clinical referral and practice patterns. Eight participants were in CHD group 1, 25 were in group 2, and 27 were in group 3. The serum creatinine level ranged from 0.2 to 1.3 mg/dL.

Technical Implementation

Implementation data are summarized in Table 1. All three sites used technologists with experience in cardiovascular MRI, and younger participants were scanned under general anesthesia. The 3D isotropic spatial resolution varied from 0.6 to 1.3 mm and was dependent on patient size. Depending on the number of cardiac phases and spatial resolution, the mean image acquisition time (\pm standard deviation) for 4D MUSIC was 12 minutes \pm 3. Relative to the local institutional MRI standard of care, the 4D MUSIC pulse sequence reduced image acquisition time for evaluation of cardiac function and vascular connections (mean, 44 minutes \pm 20 vs 12 minutes \pm 3, respectively; $P < .001$) across all centers. The local standard of care for pediatric CHD MRI involves physician supervision of image acquisition, im-

age postprocessing in some cases, and physician image interpretation. Implementation of 4D MUSIC MRI reflected a time savings of approximately 32 minutes because the need for physician supervision during image acquisition was minimized (Table 1). Use of 4D MUSIC MRI did not alter the image postprocessing time for quantification of cardiac function or physician interpretation time. On the basis of the slope of the signal intensity profile at the lung-diaphragm-liver interface as a proxy for consistent diaphragmatic relaxation (respiratory motion), respiratory control at each site varied (mean: 0.33 ± 0.22 for site 1, 0.55 ± 0.17 for site 2, and 0.52 ± 0.14 for site 3; $P = .012$).

Image Quality and Diagnostic Confidence

Figure 2 summarizes the diagnostic image quality of 4D MUSIC MRI examinations. On the basis of a five-point Likert scale, with 5 indicating excellent diagnostic quality and no artifacts, 93% of examinations (56 of 60) had image quality scores of good or excellent (mean score: 4.3 ± 0.6 for site 1, 4.9 ± 0.3 for site 2, and 4.6 ± 0.7 for site 3; $P < .001$). The mean overall image quality score across all three sites was 4.6 ± 0.2 , and the mean overall artifact score was 1.7 ± 0.3 . Artifact scores (mean score: 2.1 ± 0.7 for site 1, 1.3 ± 0.6 for site 2, and 1.6 ± 0.9 for site 3; $P < .001$) were inversely related to

Table 3: Participant Characteristics (n = 60)

Characteristic	Site 1 (n = 20 of 33)	Site 2 (n = 20 of 221)	Site 3 (n = 20 of 206)
Median age (y)*	3.6 (1.9–7.7)	0.5 (0.2–1.5)	0.5 (0.01–2.4)
Female participants	10 (50)	11 (55)	12 (60)
Median weight (kg)*	15.3 (12.6–20.1)	5.8 (4.4–10.8)	3.8 (2.9–17.6)
Ferumoxytol dose (mg/kg)	3	4	4
Indication [†]			
Group 1 [‡]	4	3	1
Group 2 [‡]	7	14	4
Group 3 [‡]	9	3	15

Note.—Unless otherwise specified, data are numbers of participants, with percentages in parentheses.

* Numbers in parentheses are the interquartile range.

[†] Congenital heart disease (CHD) diagnoses were divided into three subtypes, as follows: group 1, simple CHD (native and/or repaired, with patient cared for by the general medical community); group 2, CHD of moderate severity (with patient seen periodically at regional CHD centers); and group 3, CHD of great complexity (with patient seen regularly at quaternary CHD centers) (12).

[‡] Representative diagnoses were as follows: group 1, partial anomalous pulmonary venous return, atrial septal defect, aortic arch hypoplasia; group 2 (sinus venosus atrial septal defect, perimembranous ventricular septal defect, total anomalous pulmonary venous return, vascular rings and/or coarctation); group 3 (interrupted aortic arch, tetralogy of Fallot and variants, transposition of the great arteries, double outlet right ventricle, hypoplastic left heart syndrome, and double inlet left ventricle).

image quality scores ($r = -0.88$, $P < .001$) and respiratory motion suppression (mean signal intensity slope: 0.31 ± 0.19 for site 1, 0.55 ± 0.12 for site 2, and 0.52 ± 0.10 for site 3; $P < .001$, $r = -0.45$). In a regression model (study site, magnet field strength, image quality, image artifacts, lung-diaphragm-liver signal intensity slope), study site and magnet field strength had no effect on the outcomes ($P = .77$; 95% CI: -2.10 , 1.57). In 80% of examinations (48 of 60), the semilunar (aortic, pulmonary) and atrioventricular (mitral, tricuspid) valvular apparatus as well as leaflet thickening and motility were evaluable in all cardiac phases. Similarly, the third-order tributaries of the hepatic veins could be clearly visualized in 87% of examinations (52 of 60) and both third-order branches and tributaries of the pulmonary arteries and veins could be clearly visualized in 77% of examinations (46 of 60). In 80% of examinations (48 of 60), the coronary origins and course were clearly visualized. There was variation in image quality and motion artifacts among the sites, but all examinations were of diagnostic quality (scores of 3 or greater).

Figure 3 summarizes diagnostic confidence for normal ($n = 584$) and abnormal ($n = 196$) anatomy. On the basis of a five-point Likert scale, with 5 representing “definite” confidence, the level of diagnostic certainty for classifying abnormal versus normal intracardiac and vascular connections was high, with 730 of 780 (94%) intracardiac and vascular connections receiving a score of 4 (high) or 5 (definite). The diagnostic confidence was high or definite in 91% of structures classified as abnormal (179 of 196) and 94% of structures classified as normal (551 of 584). The diagnostic confidence for classifying normal versus abnormal anatomy was high or definite in 98% (59 of 60 examinations) of aortopulmonary connections, 95% (57 of 60 examinations) of pulmonary venous connections, and 65% (39 of 60 examinations) of coronary arteries. In one case in which the origin of the right coronary artery was not well demonstrated with 4D MUSIC, echocardiography enabled identification of

the proximal origin. In two cases involving incomplete evaluation of the coronary arteries, catheterization showed that the origin of the right coronary artery was above the sinotubular junction in one and only a single coronary artery was present in the other. Owing to stent material, metallic artifacts in one 4D MUSIC examination reduced the confident evaluation of pulmonary artery stent patency; echocardiography with Doppler imaging confirmed the patency of the stent. In 95% of MRI examinations (57 of 60), the general diagnosis was consistent with available clinical data including operative reports ($n = 36$) and imaging findings (modality: cardiac US [$n = 60$], fluoroscopic angiography [$n = 30$]). In 15 examinations, 4D MUSIC MRI findings were additive to other available imaging data. Because of the unrestricted field of view afforded by 4D MUSIC relative to echocardiography, additional information about extracardiac vascular and noncardiovascular structures, which is valuable for presurgical planning, was available in all cases.

Figures 4–6 and Movie 1 (online) provide illustrative comparisons of cases at 1.5 T and 3.0 T, in male and female children (age range, 12 days to 12 years; weight range, 3.6–28 kg). Investigators graded the examinations in Figures 4–6 as having excellent image quality and minimal to mild artifacts. A spectrum of complex intracardiac morphologic features and vascular geometry was clearly depicted. In participants with pulmonary artery stent and/or graft material (Fig 5) or conduits (Fig 6), the vascular lumen was well demonstrated with minor signal intensity loss. Even in images with lower image quality and higher artifact scores, the examinations had acceptable diagnostic confidence. Movie 2 (online) provides illustrative cases with lower image quality scores of 2.5–4 and higher artifact scores of 3–4.

The correlation between 4D MUSIC– and 2D bSSFP–derived ventricular volumes and ejection fractions across all sites was high (Spearman rank correlation, 0.72 – 0.85 ; $P < .001$ for all). The mean biases between 2D bSSFP– and 4D

Diagnostic image quality and artifacts

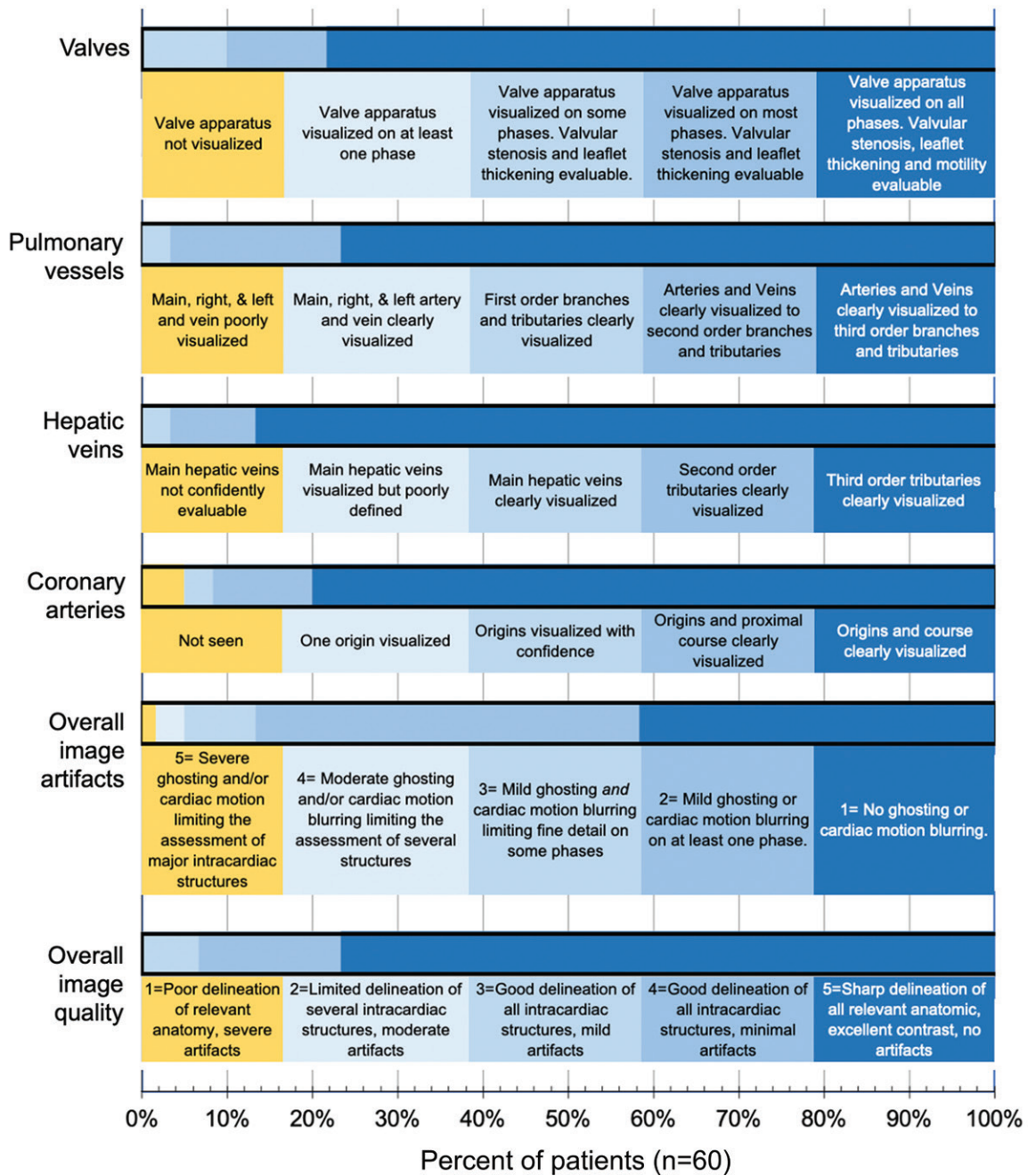


Figure 2: Histogram shows multisite image quality for four-dimensional multiphase steady-state imaging with contrast enhancement MRI with use of ferumoxytol. Summary of image quality and artifact scores is shown (60 examinations, core laboratory scoring). Image quality and artifact scoring criteria for each parameter are provided beneath respective color bar, and color scale reflects percentage of examinations. Image quality score is inversely related to artifact score. A maximal image quality score of 5 reflects sharp delineation of all relevant anatomic structures, excellent contrast, and no artifacts, whereas an artifact score of 1 reflects no ghosting or cardiac motion blurring. Structures such as valves as well as pulmonary, hepatic, and coronary vessels are evaluated on a continuum of fine detail reflected by the five-point scale.

MUSIC-derived volumes and ejection fractions were narrow for the left ventricle and wider for the right ventricle, with a mean bias of 4.1 mL/m² (95% CI: -10.9, 2.6) for left ventricle end-diastolic volume, 0.6 mL/m² (95% CI: -2.0, 3.3) for left ventricle end-systolic volume, 1.6% (95% CI: -4.0, 0.7) for left ventricle ejection fraction, 16

mL/m² (95% CI: 5.5, 26.7) for right ventricle end-diastolic volume, 3.3 mL/m² (95% CI: -4.3, 10.9) for right ventricle end-systolic volume, and 1.8% (95% CI: -1.0, 4.7) for right ventricle ejection fraction. Factors affecting underestimation of right ventricle end-diastolic volume may have included variation in basal section selection and temporal

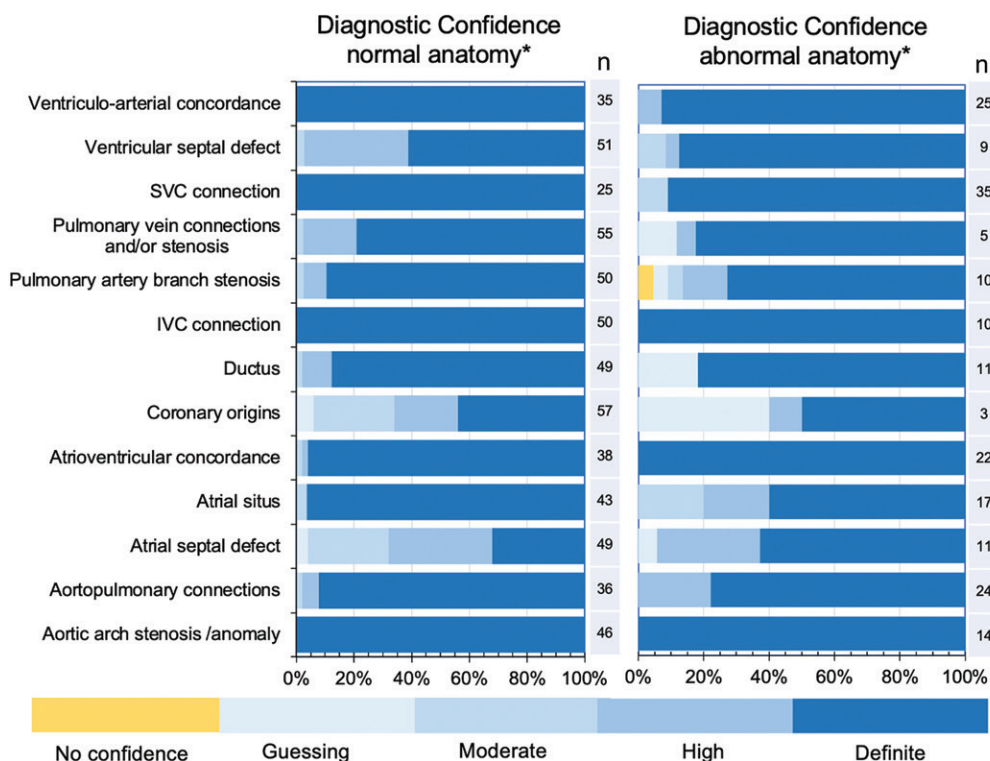


Figure 3: Histogram shows multisite diagnostic confidence for four-dimensional multiphase steady-state imaging with contrast enhancement MRI with ferumoxytol. Image summarizes diagnostic confidence scores for 13 categories of normal and abnormal findings (60 examinations, 780 morphologic connections, locally scored [*]). Diagnostic confidence was graded on scale of 1 to 5 (1 = no confidence, 2 = guessing, 3 = moderate, 4 = high, 5 = definite). IVC = inferior vena cava, SVC = superior vena cava.

resolution, but the difference did not reach statistical significance ($P = .49$).

Discussion

Conventional MRI in pediatric congenital heart disease (CHD) is associated with long examination times, a requirement for specialized physician supervision, and lack of standard acquisition protocols due to a wide variation in cardiovascular anomalies. In a previous single-center study of four-dimensional (4D) multiphase steady-state MRI using ferumoxytol and the multiphase steady-state imaging with contrast enhancement (MUSIC) pulse sequence (6), diagnostic image quality was high (10,11). Our early multicenter results confirmed that 4D MUSIC MRI provides reliable high-quality images, across multiple sites and field strengths, with use of a simple acquisition protocol ($P = .77$; 95% CI: $-2.10, 1.57$). In 93% of examinations (56 of 60), image quality scores were good or excellent. Artifact scores were inversely related to image quality scores ($r = -0.88, P < .001$) and respiratory motion suppression ($r = -0.45; P < .001$). Diagnostic confidence was rated as high or definite in 730 of the 780 (94%) intracardiac and vascular connections. Ventricular volumes and ejection fraction showed high correlation with standard two-dimensional cine ($r = 0.72-0.85, P < .001$). At all sites, 4D MUSIC MRI shortened the cine and angiographic image acquisition time relative to the prior CHD MRI acquisition protocol (mean, 12 minutes ± 3 vs 44 minutes ± 20 , respectively; $P < .001$), reduced the need for specialist physician supervision during

image acquisition, and alleviated concerns about gadolinium retention. These findings have implications for standardizing MRI in pediatric CHD.

The emergence of 4D MRI techniques (6,7,15-19) has transformed image acquisition in CHD. By generating dynamic, multiphase, 3D high-spatial-resolution (0.6-0.9 mm isotropic, without interpolation) images with inline reconstruction, 4D MUSIC has replaced the pre-existing iterative, customized 2D acquisition process with a simple volumetric acquisition that captures all relevant dynamic anatomy, irrespective of disease complexity. Because of its Cartesian k-space trajectory and immediate inline reconstruction, 4D MUSIC is readily implemented on standard MRI systems. Whereas 3.0 T has inherent signal-to-noise advantages over 1.5 T, the higher relaxivity of ferumoxytol at a lower field strength can partially offset the discrepancy, as suggested by the high image quality scores at sites 1 (mean score, 4.3 ± 0.6) and 2 (mean score, 4.9 ± 0.3), which performed imaging at 1.5 T.

Two recent alternative approaches to 4D acquisition merit further discussion: whole-heart 4D bSSFP cine (2) and 4D flow imaging (1). A whole-heart, gadolinium-enhanced, 4D bSSFP technique proposed by Moghari et al (2) is a free-breathing method that relies on a periodically acquired k-space center line for prospective respiratory motion compensation and uses a centric profile ordering to fill k-space. An isotropic spatial resolution of $2 \times 2 \times 2 \text{ mm}^3$ with 20 cardiac phases (interpolated to 30 phases) was achievable within 5.9 minutes. There is merit in having a free-breathing technique, but in young children, being within an MRI

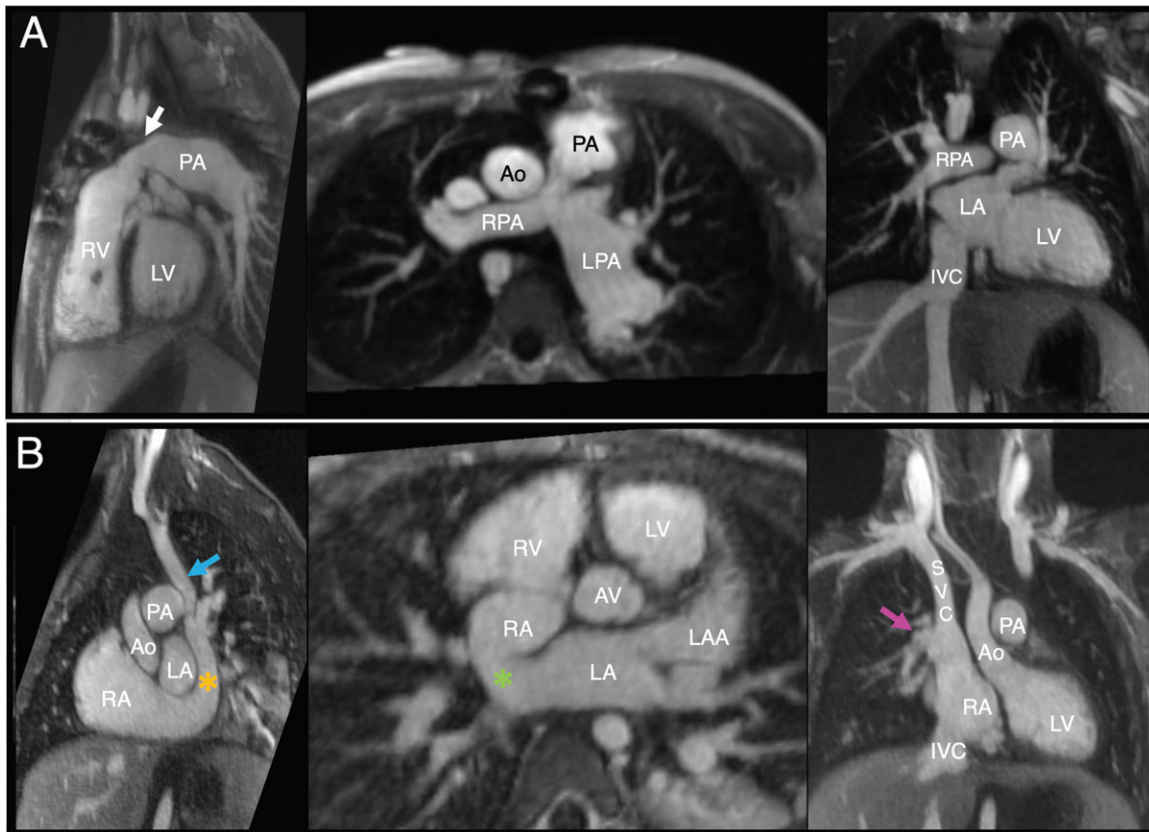


Figure 4: MRI scans obtained by using the four-dimensional multiphase steady-state imaging with contrast enhancement pulse sequence from site 1 (1.5 T, 4 mg/kg ferumoxytol). Images are shown in arbitrary imaging planes that best depict normal and abnormal anatomy. Ao = aorta, IVC = inferior vena cava, LV = left ventricle, PA = pulmonary artery, RV = right ventricle. A, Multiplanar reformatted images in a 9-year-old boy (weight, 21.4 kg) with Fallot-type absent pulmonic valve syndrome after closure of a ventricular septal defect shows narrowing of right ventricle to pulmonary artery conduit (arrow). The left pulmonary artery (LPA) is severely dilated. RPA = right pulmonary artery. B, Multiplanar reformatted images in 3-year-old boy (weight, 14 kg) with sinus venosus atrial septal defect (green asterisk), left persistent superior vena cava (SVC) (blue arrow) to coronary sinus (orange asterisk), and partial anomalous pulmonary venous return of right upper vein and middle branch of right lower vein to superior vena cava (pink arrow). AV = aortic valve, LA = left atrium, LAA = left atrial appendage, RA = right atrium. Both patient images received overall quality scores of 5 and artifact scores of 1.5.

environment for any period of time may be anxiety provoking (20) and some form of sedation is likely needed. This fact was borne out by the experience of Moghari et al (2), who found that the 3D image quality was lower than 2D image quality. In our study, when motion was not fully suppressed during MRI, then the diagnostic quality was undermined to some degree owing to the loss in fine detail, as evidenced by higher artifact scores (mean score: 2.1 ± 0.7 at site 1, 1.3 ± 0.6 at site 2, and 1.6 ± 0.9 at site 3; $P < .001$) secondary to motion (mean score: 0.31 ± 0.19 at site 1, 0.55 ± 0.12 at site 2, and 0.52 ± 0.10 at site 3; $P < .001$, $r = -0.45$).

The ferumoxytol-enhanced 4D flow strategy proposed by Cheng et al (1) uses intrinsic navigators with velocity-encoding gradients for flow sensitivity and compressed sensing for the acceleration of image acquisition. The basic building block for 4D MUSIC and conventional 4D flow imaging is a spoiled gradient echo. With MUSIC, the pulse sequence structure is similar to that of contrast-enhanced MR angiography and is insensitive to off-resonance artifact, requiring 3 msec or less per k-space line. For 4D flow, additional gradient lobes are required within each repetition (repetition time cycle) for directional velocity encoding, which may prolong the minimum repetition time by

40%–80% (21), with a proportional increase in imaging time per k-space line. Four repetitions of the complete volumetric acquisition are required for 4D flow encoding, resulting in acquisition times six to eight times that for MUSIC with similar resolution and undersampling. Whereas our 4D MUSIC acquisition used only data acquired during the expiratory (quiescent) phase of respiration and rejected the rest, Cheng et al (1) used respiratory reordering whereby the full respiratory cycle was used for image reconstruction. Analogous to respiratory ordered phase encoding (22), the approach proposed by Cheng et al to diminish visible respiratory motion artifact may introduce a loss of resolution in fine anatomic detail at the cost of providing flow data.

The practical, real-world attributes of 4D MUSIC MRI with ferumoxytol have high value because clinical management decisions in patients with CHD frequently hinge on findings at the time of imaging. The use of ferumoxytol, however, must be weighed against other factors. In its on-label indication as an intravenous therapeutic, ferumoxytol carries a warning regarding potential acute hypersensitivity reactions associated with rapid bolus injection, and slow infusion is recommended. For off-label diagnostic use, recent work from a multicenter observational

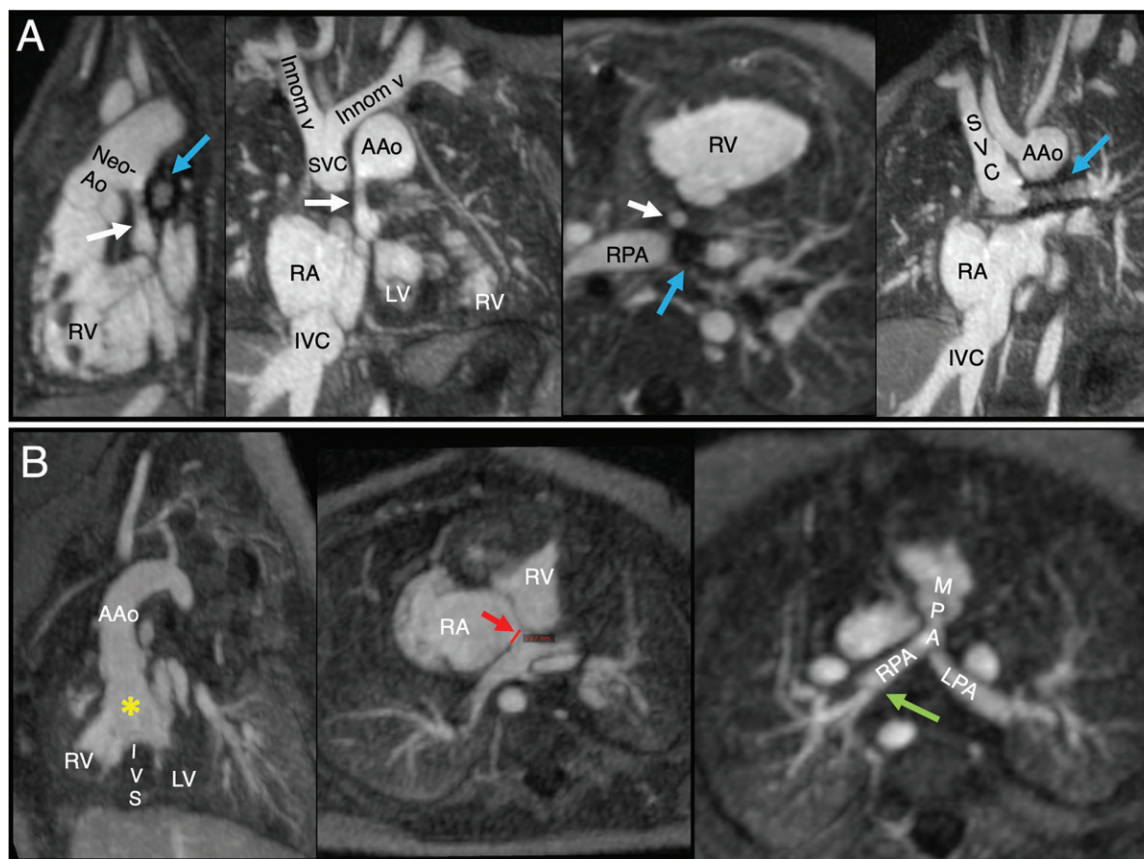


Figure 5: MRI scans acquired by using the four-dimensional multiphase steady-state imaging with contrast enhancement pulse sequence from site 2 (1.5 T, 4 mg/kg ferumoxytol). Images are shown in arbitrary imaging planes that best depict normal and abnormal anatomy. AAo = ascending aorta, LV = left ventricle, RA = right atrium, RPA = right pulmonary artery, RV = right ventricle. **A**, Multiplanar reformatted images in full-term 3-year-old boy (weight, 17 kg) with hypoplastic left heart syndrome (mitral stenosis and aortic atresia) who was initially palliated with stage I Norwood procedure that included right ventricle–pulmonary artery conduit. He subsequently underwent superior cavopulmonary anastomosis with takedown of right ventricle–pulmonary artery conduit. Postoperatively, he required stent placement (blue arrow, 7.6 mm) of central pulmonary artery owing to long segment stenosis. Artifacts from stent material are present with clear visualization of pulmonary arterial lumen (blue arrow). The neo-aorta (Neo-Ao) (resulting from fusion of hypoplastic native aorta [white arrows, 5.2 × 5.2 mm]) with portion of the main pulmonary artery and native aorta are clearly depicted. Innom v = innominate vein, IVC = inferior vena cava, SVC = superior vena cava. **B**, Multiplanar reformatted images in full-term 4.7-month-old girl (weight, 5.8 kg) with tetralogy of Fallot, complete atrioventricular canal defect (yellow asterisk = inlet ventricular septal defect; red arrow = primum atrial septal defect, 3.3 mm), and branch pulmonary artery stenosis with hypoplasia (green arrow). MPA = main pulmonary artery. For both patients, images received an overall quality score of 5 and an artifact score of 1.

registry consisting of 4240 ferumoxytol injections (14) revealed no serious adverse reactions. Off-label diagnostic ferumoxytol use should adhere to U.S. Food and Drug Administration recommendations, including dilution, slow injection, and monitoring of vital signs during and after injection for up to 30 minutes. At the time of writing, ferumoxytol is marketed only in the United States, and for now this limits its more widespread use.

Our study had limitations. First, we sampled only 13% of the available pool of examinations (60 of 460), and the scope of our study was limited to pediatric patients with CHD who underwent 4D MUSIC MRI under general anesthesia. Second, the 4D MUSIC technique relies on regularity and adequate control of the respiratory waveform during mechanical ventilation. Therefore, the image quality will reflect how well both cardiac and respiratory motion artifacts are eliminated. In most patients, if the depth of sedation is adequate and neuromuscular blockade is active, respiratory motion suppression is excellent. If, however, 4D MUSIC is performed when the

effect of muscle relaxants is wearing off and the depth of anesthesia has lightened, the images will be prone to artifacts. Third, in pediatric CHD MRI, a balance between spatial resolution, temporal resolution, and imaging time is necessary. The range of temporal resolution (20–45 msec) relative to the modest number of cardiac phases achieved across the three centers reflects a balance between the high heart rate range that is typical in very small children and the total image acquisition time. As implemented in this work, the 4D MUSIC technique uses only modest levels of data under-sampling by leveraging parallel acquisition without data sharing or interpolation to attain true isotropic 3D resolution. Although current specifications clearly meet the requirements for highly diagnostic studies, much potential remains for image acceleration and reconstruction techniques that can further improve performance. Successful implementation of high-spatial-resolution, sedation-only, or anesthesia-free 4D imaging remains the subject of active research in our laboratory and others, but the clinical

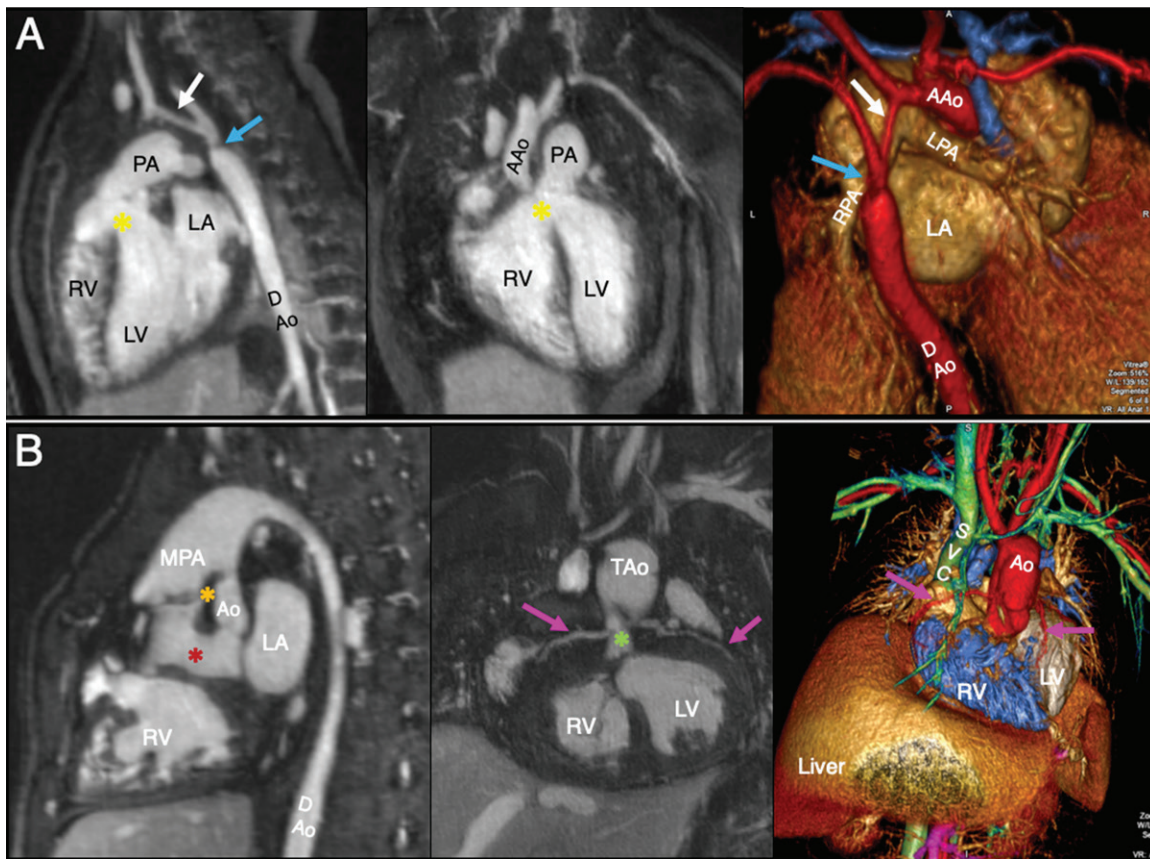


Figure 6: MRI scans acquired by using the four-dimensional (4D) multiphase steady-state imaging with contrast enhancement pulse sequence from site 3 (3.0 T, 4 mg/kg ferumoxytol). Images are shown in arbitrary imaging planes that best depict normal and abnormal anatomy. LA = left atrium, LV = left ventricle, RV = right ventricle. **A**, Multiplanar reformatted and three-dimensional (3D) color volume-rendered images in 12-day-old girl (weight, 3.6 kg) with ventricular septal defect (yellow asterisks), transverse arch hypoplasia (white arrows), and aortic coarctation (blue arrows). Overall image quality score was 4, and artifact score was 2. Three-dimensional color volume-rendered image is shown in bird's eye view and clearly depicts 3D spatial relationships between cardiac anatomy and vascular connections. AAo = ascending aorta, D Ao = descending aorta, LPA = left pulmonary artery, PA = pulmonary artery, RPA = right pulmonary artery. **B**, Multiplanar reformatted and 3D color volume-rendered images in 9-year-old girl (weight, 28 kg) with DiGeorge syndrome with interrupted aortic arch (type B) and ventricular septal defect who was initially palliated with arch repair, Damus-Kay-Stansel procedure (anastomosis of main pulmonary artery [MPA] to hypoplastic ascending aorta [orange asterisk], Movie 1A [online]), and right ventricle to pulmonary artery conduit placement. At 9 months of age, she underwent Rastelli operation consisting of baffle closure of ventricular septal defect to neo-aortic valve (red asterisk), and homograft right ventricle–pulmonary artery conduit placement. During the next several years, she required subsequent conduit replacements. Both coronary arteries originate from hypoplastic native aorta (Ao) (green asterisk, 1.5 cm at sinotubular junction), and proximal course of right and left coronary artery systems (pink arrows) are well demonstrated. Right ventricle hypertrophy is present. Three-dimensional color volume-rendered image is available in 4D mode as Movie 1B (online). Overall image quality score was 5, and artifact score was 1. TAo = transverse aorta.

performance and reliability of such techniques have not yet been established, and these were not the subject of our current study.

In conclusion, our initial multicenter results established that four-dimensional (4D) multiphase steady-state imaging with contrast enhancement (MUSIC) cardiovascular MRI was feasible in pediatric patients with congenital heart disease (CHD) across institutions, field strengths, age spectrum, and disease complexity. Four-dimensional MUSIC MRI consistently achieved reliable diagnostic images and highly valued quality measures with respect to time efficiency, simplification of image acquisition, and alleviation of concerns about gadolinium retention or renal function. More widespread multicenter experience will be helpful for definitive evaluation of 4D MUSIC MRI in CHD. A prospective randomized study across centers with and without high-level subspecialty skills in cardiovascular MRI is needed for more complete

evaluation of the clinical impact of simplified, standardized, image-based care in complex pediatric CHD.

Author contributions: Guarantors of integrity of entire study, K.L.N., J.P.E.; study concepts/study design or data acquisition or data analysis/interpretation, all authors; manuscript drafting or manuscript revision for important intellectual content, all authors; approval of final version of submitted manuscript, all authors; agrees to ensure any questions related to the work are appropriately resolved, all authors; literature research, K.L.N., A.B., K.K.W., P.H., J.P.E.; clinical studies, R.M.G., L.M.G., A.B., C.K.R., M.A.F., K.K.W., P.H., J.P.E.; experimental studies, C.K.R., P.H.; statistical analysis, K.L.N.; and manuscript editing, all authors

Disclosures of Conflicts of Interest: K.L.N. disclosed no relevant relationships. R.M.G. disclosed no relevant relationships. L.M.G. disclosed no relevant relationships. T.Y. disclosed no relevant relationships. A.B. disclosed no relevant relationships. C.K.R. disclosed no relevant relationships. M.A.F. disclosed no relevant relationships. K.K.W. disclosed no relevant relationships. P.H. Activities related to the present article: disclosed no relevant relationships. Activities not

related to the present article: disclosed no relevant relationships. Other relationships: is an inventor of U.S. patent US10517491B2, which is currently assigned to the Regents of the University of California. **J.P.F.** Activities related to the present article: disclosed no relevant relationships. Activities not related to the present article: disclosed no relevant relationships. Other relationships: is an inventor of U.S. patent US10517491B2, which is currently assigned to the Regents of the University of California.

References

- Cheng JY, Hanneman K, Zhang T, et al. Comprehensive motion-compensated highly accelerated 4D flow MRI with ferumoxytol enhancement for pediatric congenital heart disease. *J Magn Reson Imaging* 2016;43(6):1355–1368.
- Moghari MH, Barthur A, Amaral ME, Geva T, Powell AJ. Free-breathing whole-heart 3D cine magnetic resonance imaging with prospective respiratory motion compensation. *Magn Reson Med* 2018;80(1):181–189.
- Usman M, Ruijsink B, Nazir MS, Cruz G, Prieto C. Free breathing whole-heart 3D CINE MRI with self-gated Cartesian trajectory. *Magn Reson Imaging* 2017;38:129–137.
- Kozak BM, Jaimes C, Kirsch J, Gee MS. MRI Techniques to Decrease Imaging Times in Children. *RadioGraphics* 2020;40(2):485–502.
- Bustin A, Fuin N, Botnar RM, Prieto C. From Compressed-Sensing to Artificial Intelligence-Based Cardiac MRI Reconstruction. *Front Cardiovasc Med* 2020;7:17.
- Han F, Rapacchi S, Khan S, et al. Four-dimensional, multiphase, steady-state imaging with contrast enhancement (MUSIC) in the heart: a feasibility study in children. *Magn Reson Med* 2015;74(4):1042–1049.
- Han F, Zhou Z, Han E, et al. Self-gated 4D multiphase, steady-state imaging with contrast enhancement (MUSIC) using rotating cartesian K-space (ROCK): validation in children with congenital heart disease. *Magn Reson Med* 2017;78(2):472–483.
- Finn JP, Nguyen KL, Hu P. Ferumoxytol vs. Gadolinium agents for contrast-enhanced MRI: Thoughts on evolving indications, risks, and benefits. *J Magn Reson Imaging* 2017;46(3):919–923.
- Bashir MR, Bhatti L, Marin D, Nelson RC. Emerging applications for ferumoxytol as a contrast agent in MRI. *J Magn Reson Imaging* 2015;41(4):884–898.
- Nguyen KL, Han F, Zhou Z, et al. 4D MUSIC CMR: value-based imaging of neonates and infants with congenital heart disease. *J Cardiovasc Magn Reson* 2017;19(1):40.
- Zhou Z, Han F, Rapacchi S, et al. Accelerated ferumoxytol-enhanced 4D multiphase, steady-state imaging with contrast enhancement (MUSIC) cardiovascular MRI: validation in pediatric congenital heart disease. *NMR Biomed* 2017;30(1):e3663.
- Nguyen KL, Yoshida T, Han F, et al. MRI with ferumoxytol: a single center experience of safety across the age spectrum. *J Magn Reson Imaging* 2017;45(3):804–812.
- Everett AD. Cove Point Foundation: Helen B Taussig Children's Heart Center, Johns Hopkins University. <http://www.pted.org/?id=overview1>. Accessed November 6, 2017.
- Nguyen KL, Yoshida T, Kathuria-Prakash N, et al. Multicenter Safety and Practice for Off-Label Diagnostic Use of Ferumoxytol in MRI. *Radiology* 2019;293(3):554–564.
- Kressler B, Spincemaille P, Nguyen TD, et al. Three-dimensional cine imaging using variable-density spiral trajectories and SSFP with application to coronary artery angiography. *Magn Reson Med* 2007;58(3):535–543.
- Liu J, Spincemaille P, Codella NC, Nguyen TD, Prince MR, Wang Y. Respiratory and cardiac self-gated free-breathing cardiac CINE imaging with multiecho 3D hybrid radial SSFP acquisition. *Magn Reson Med* 2010;63(5):1230–1237.
- Liu J, Nguyen TD, Zhu Y, et al. Self-gated free-breathing 3D coronary CINE imaging with simultaneous water and fat visualization. *PLoS One* 2014;9(2):e89315.
- Coppo S, Piccini D, Bonanno G, et al. Free-running 4D whole-heart self-navigated golden angle MRI: initial results. *Magn Reson Med* 2015;74(5):1306–1316.
- Vasanawala SS, Hanneman K, Alley MT, Hsiao A. Congenital heart disease assessment with 4D flow MRI. *J Magn Reson Imaging* 2015;42(4):870–886.
- Maliszka KL, Martin T, Shiloff D, Yu DC. Reactions of young children to the MRI scanner environment. *Magn Reson Med* 2010;64(2):377–381.
- Wang D, Shao J, Ennis DB, Hu P. Phase-contrast MRI with hybrid one and two-sided flow-encoding and velocity spectrum separation. *Magn Reson Med* 2017;78(1):182–192.
- Bailes DR, Gilderdale DJ, Bydder GM, Collins AG, Firmin DN. Respiratory ordered phase encoding (ROPE): a method for reducing respiratory motion artefacts in MR imaging. *J Comput Assist Tomogr* 1985;9(4):835–838.